

Dispersion-Controlled Thermal Degradation Kinetics of PMMA/NiFe₂O₄ Nanocomposites Prepared with Different Mixing Times

Aytekin ULUTAŞ^{1*} 

¹Balikesir University, Edremit Civil Aviation College, Department of Aviation Management, Balikesir, Turkey

Article Info

Research article
Received: 18/12/2025
Revision: 16/02/2026
Accepted: 20/02/2026

Keywords

Poly(methyl methacrylate)
Thermal analysis
NiFe₂O₄
Activation energy Kissinger
Ozawa
Augis-Bennett

Makale Bilgisi

Araştırma makalesi
Başvuru: 18/12/2025
Düzelme: 16/02/2026
Kabul: 20/02/2026

Anahtar Kelimeler

Polimetil metakrilat
Termal analiz
NiFe₂O₄
Aktivasyon enerjisi
Kissinger
Ozawa
Augis-Bennett

Graphical/Tabular Abstract (Grafik Özet)

This study demonstrates that peak thermal stability in PMMA/NiFe₂O₄ nanocomposites is achieved through optimum dispersion (partial agglomeration) rather than maximum homogeneity. / Bu çalışma, PMMA/NiFe₂O₄ nanokompozitlerinde en yüksek ısı direncinin tam homojen dağılımla değil, kısmi topaklanma (optimum dağılım) ile elde edildiğini kanıtlamaktadır.

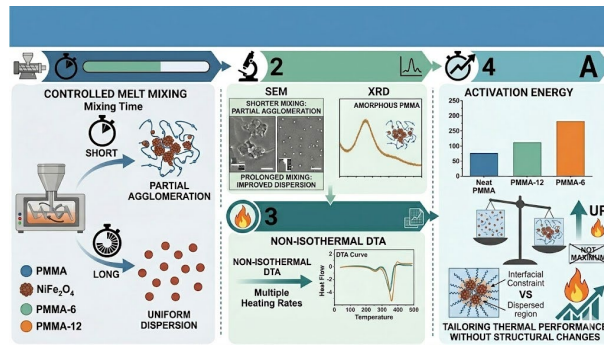


Figure A: Thermal degradation kinetics of PMMA/NiFe₂O₄ nanocomposites /Şekil A: PMMA/NiFe₂O₄ nanokompozitlerinin termal bozunma kinetiği

Highlights (Önemli noktalar)

- PMMA/NiFe₂O₄ nanocomposites were prepared via controlled melt mixing to study dispersion effects. / PMMA/NiFe₂O₄ nanokompozitleri, dağılım etkilerini incelemek için kontrollü eriyik karıştırma yoluyla hazırlanmıştır.
- Nanoparticle dispersion was systematically controlled by varying the mixing duration. / Nanoparçacık dağılımı, karıştırma süresi değiştirilerek sistematik olarak kontrol edilmiştir.
- Maximum thermal stability was observed at an optimum dispersion state rather than maximum homogeneity. / Maksimum termal kararlılık, maksimum homojenlik yerine optimum bir dağılım durumunda gözlemlenmiştir.
- PMMA-6 exhibited the highest activation energy due to enhanced interfacial constraints. / PMMA-6, artan arayüzey kısıtlamaları nedeniyle en yüksek aktivasyon enerjisini sergilemiştir.

Aim (Amaç): To systematically investigate the effect of nanoparticle dispersion states, controlled by melt mixing time, on the thermal degradation kinetics of PMMA/NiFe₂O₄ nanocomposites. / Eriterek karıştırma süresiyle kontrol edilen nanoparçacık dağılım durumlarının PMMA/NiFe₂O₄ nanokompozitlerinin termal bozunma kinetiği üzerindeki etkisini sistematik olarak incelemek.

Originality (Özgünlük): Optimum dispersion with partial agglomeration provides superior thermal resistance, challenging the assumption that maximum dispersion yields peak performance. / Kısmi topaklanma içeren optimum dağılım, maksimum dağılım varsayımını sorgulayarak daha yüksek termal direnç sağlar.

Results (Bulgular): XRD confirmed an amorphous matrix; partially agglomerated PMMA-6 showed the highest activation energy, 30% above neat PMMA. / XRD amorf matrisi doğrulamış; kısmi topaklanmalı PMMA-6, saf PMMA'dan %30 daha yüksek aktivasyon enerjisi göstermiştir.

Conclusion (Sonuç): Thermal degradation in these nanocomposites is governed by an optimum dispersion state where interfacial constraints are maximized, rather than by achieving perfect homogeneity. / Bu nanokompozitlerdeki termal bozunma, mükemmel homojenliğe ulaşmaktan ziyade, arayüzey kısıtlamalarının maksimize edildiği optimum bir dağılım durumu tarafından yönetilmektedir.



Dispersion-Controlled Thermal Degradation Kinetics of PMMA/NiFe₂O₄ Nanocomposites Prepared with Different Mixing Times

Aytekin ULUTAŞ^{1*}

¹Balikesir University, Edremit Civil Aviation College, Department of Aviation Management, Balıkesir, Turkey

Article Info

Research article
Received: 18/12/2025
Revision: 16/02/2026
Accepted: 20/02/2026

Keywords

Poly(methyl methacrylate)
Thermal analysis
NiFe₂O₄
Activation energy
Kissinger
Ozawa
Augis-Bennett

Abstract

The thermal degradation behavior of polymer nanocomposites is strongly governed by nanoparticle dispersion; however, the relationship between dispersion homogeneity and degradation kinetics remains unclear. In this study, PMMA/NiFe₂O₄ nanocomposites were prepared via controlled melt mixing with varying mixing times to systematically investigate the effect of dispersion state on thermal degradation kinetics. Structural and morphological characterization was carried out using X-ray diffraction (XRD) and scanning electron microscopy (SEM), while non-isothermal differential thermal analysis (DTA) was employed at multiple heating rates to evaluate degradation behavior. XRD results confirmed that the incorporation of NiFe₂O₄ nanoparticles did not alter the amorphous structure of the PMMA matrix. SEM analysis revealed that prolonged mixing significantly improved nanoparticle dispersion, whereas shorter mixing resulted in partial agglomeration. Despite comparable degradation peak temperatures across all samples, pronounced differences in degradation kinetics were observed. Activation energies calculated using the Kissinger, Ozawa, and Augis-Bennett methods indicated that the PMMA-6 nanocomposite exhibited the highest activation energy (~270 kJ/mol), approximately 30% higher than neat PMMA and ~25% higher than the more homogeneously dispersed PMMA-12 sample. These results indicate that maximum nanoparticle dispersion does not necessarily correspond to maximum thermal resistance. Instead, an optimum dispersion state characterized by partial agglomeration and enhanced interfacial constraint governs the thermal degradation kinetics of PMMA/NiFe₂O₄ nanocomposites. This study highlights the critical role of processing-controlled dispersion in tailoring the thermal performance of polymer nanocomposites without inducing structural changes.

Farklı Karıştırma Süreleriyle Hazırlanan PMMA/NiFe₂O₄ Nanokompozitlerinde Dağılım Kontrollü Termal Bozunma Kinetiği

Makale Bilgisi

Araştırma makalesi
Başvuru: 18/12/2025
Düzeltilme: 16/02/2026
Kabul: 20/02/2026

Anahtar Kelimeler

Poli(metil metakrilat)
Termal analiz
NiFe₂O₄
Aktivasyon enerjisi
Kissinger
Ozawa
Augis-Bennett

Öz

Polimer nanokompozitlerin termal bozunma davranışı büyük ölçüde nanoparçacık dağılımı tarafından belirlenmektedir; ancak dağılım homojenliği ile bozunma kinetiği arasındaki ilişki henüz tam olarak açıklığa kavuşmamıştır. Bu çalışmada, farklı karıştırma süreleri kullanılarak kontrollü ergiyik karıştırma yöntemiyle hazırlanan PMMA/NiFe₂O₄ nanokompozitlerinde dağılım durumunun termal bozunma kinetiği üzerindeki etkisi sistematik olarak incelenmiştir. Yapısal ve morfolojik karakterizasyon X-ışını kırınımı (XRD) ve taramalı elektron mikroskobu (SEM) ile gerçekleştirilmiş, bozunma davranışının değerlendirilmesi için farklı ısıtma hızlarında izotermal olmayan diferansiyel termal analiz (DTA) uygulanmıştır. XRD sonuçları, NiFe₂O₄ nanoparçacık ilavesinin PMMA matrisinin amorf yapısını değiştirmediğini göstermiştir. SEM analizleri, uzun karıştırma sürelerinin nanoparçacık dağılımını belirgin şekilde iyileştirdiğini, daha kısa karıştırma sürelerinin ise kısmi aglomerasyona yol açtığını ortaya koymuştur. Tüm numunelerde bozunma pik sıcaklıkları benzer olmasına rağmen, bozunma kinetiğinde belirgin farklılıklar gözlemlenmiştir. Kissinger, Ozawa ve Augis-Bennett yöntemleri kullanılarak hesaplanan aktivasyon enerjileri, PMMA-6 nanokompozitinin en yüksek aktivasyon enerjisine (~270 kJ/mol) sahip olduğunu ve bu değerini saf PMMA'ya kıyasla yaklaşık %30, daha homojen dağılıma sahip PMMA-12 numunesine kıyasla ise yaklaşık %25 daha yüksek olduğunu göstermiştir. Elde edilen sonuçlar, maksimum nanoparçacık dağılımının her zaman maksimum termal dayanım anlamına gelmediğini ortaya koymaktadır. Bunun yerine, kısmi aglomerasyon ve artmış arayüzeyel kısıtlamalarla karakterize edilen optimum bir dağılım durumunun PMMA/NiFe₂O₄ nanokompozitlerinin termal bozunma kinetiğini belirlediği görülmüştür. Bu çalışma, yapısal değişime neden olmaksızın polimer nanokompozitlerin termal performansının ayarlanmasında işlem koşullarıyla kontrol edilen dağılımın kritik rolünü vurgulamaktadır.

1. INTRODUCTION (GİRİŞ)

The thermal degradation behavior of polymeric materials has been a subject of extensive research due to its importance in determining service performance and lifetime in various applications [1]. Among thermoplastics, polymethyl methacrylate (PMMA) has attracted considerable attention owing to its excellent optical clarity, mechanical properties, and ease of processing. However, pure PMMA exhibits limited thermal stability, which constrains its use in high-temperature or demanding environments [2,3]. One effective strategy to enhance the thermal and mechanical behavior of PMMA is the incorporation of inorganic nanoparticles into its matrix, leading to nanocomposite systems with tailored properties [4,5]. Metal oxide nanoparticles, such as titanium dioxide (TiO₂), zinc oxide (ZnO), and ferrites, have been used to reinforce PMMA due to their high thermal stability and potential to alter degradation pathways [6,7]. The addition of nanoparticles may influence not only the degradation temperature but also the kinetic mechanisms underlying the thermal decomposition processes [8].

Despite extensive studies on nanoparticle-reinforced PMMA matrices, the impact of mixing time and dispersion state on thermal degradation kinetics remains underexplored. Previous works have shown that nanoparticle dispersion within a polymer matrix significantly affects thermal stability and degradation behavior; however, the relationship between dispersion homogeneity and activation energy is not always straightforward [9,10]. For instance, optimal dispersion can provide extensive interfacial interactions that restrict polymer chain mobility, thereby increasing the energy barrier for degradation, whereas either poor dispersion or complete agglomeration can lead to alternative thermal response patterns [11,12].

In addition to structural factors, understanding the degradation kinetics is essential for predicting material behavior under thermal stress. Kinetic parameters such as activation energy (E_a) are widely used for this purpose and can be evaluated using non-isothermal methods, including Kissinger, Ozawa, and Augis–Bennett analyses [13–15]. These methods allow comparison of thermal stability of polymer and nanocomposite systems under different heating rates, and they have been applied in various polymeric matrices to elucidate the effects of nanofiller type, size, and distribution [14,16].

Despite extensive studies on nanoparticle-reinforced PMMA systems, most existing works implicitly assume that improved or maximum nanoparticle dispersion leads to enhanced thermal stability. However, the distinction between maximum dispersion and an optimum dispersion state, particularly in terms of thermal degradation kinetics and activation energy, has not been systematically addressed. In addition, the role of controlled partial agglomeration in modifying degradation energetics without altering the degradation mechanism remains unclear. Therefore, a comprehensive understanding of how processing-controlled dispersion states govern thermal degradation kinetics is still lacking in the literature.

In this study, we investigate the thermal degradation behavior and kinetics of NiFe₂O₄-reinforced PMMA nanocomposites prepared with different mixing times. Differential thermal analysis (DTA) was conducted at multiple heating rates to obtain characteristic degradation temperatures, which were then used to calculate activation energies using Kissinger, Ozawa, and Augis–Bennett methods. By correlating thermal stability and kinetic parameters with nanoparticle dispersion conditions, this work aims to provide a comprehensive understanding of how processing parameters govern the thermal performance of PMMA-based nanocomposites. This study demonstrates that optimum rather than maximum dispersion governs degradation kinetics.

2. MATERIALS AND METHODS (MATERİYAL VE METOD)

2.1. Materials (Malzemeler)

Polymethyl methacrylate (PMMA, $M_w = 35,000$ g/mol, Acros Organics) was used as the polymer matrix material in this study due to its well-documented thermal degradation behavior and widespread application in polymer nanocomposite research [17]. Nickel ferrite (NiFe₂O₄) nanoparticles (CAS No. 12168-54-6, Sigma-Aldrich, Merck KGaA, Darmstadt, Germany) were employed as the inorganic reinforcing phase owing to their high thermal stability, chemical resistance, and potential to influence polymer degradation pathways [18]. All materials were of analytical grade and used as received without further purification.

Prior to composite preparation, PMMA and NiFe₂O₄ powders were dried at 353 K for 24 h to remove residual moisture and prevent unwanted thermal effects during processing. The nanoparticle content was kept constant in all nanocomposite

samples to isolate the effect of mixing time on thermal behavior and degradation kinetics.

2.2. Preparation of PMMA/NiFe₂O₄ Nanocomposites (Preparation of PMMA/NiFe₂O₄ Nanocomposites)

PMMA/NiFe₂O₄ nanocomposites were prepared using a melt-blending procedure under controlled processing conditions. The NiFe₂O₄ nanoparticle content was fixed at 2.5 wt.% for all samples in order to isolate the effect of mixing time on dispersion and degradation behavior. Melt mixing was performed at a processing temperature of 480 K using an internal mixer (twin-screw extruder) operating at a rotational speed of 100 rpm. Two different mixing durations, 6 min and 12 min, were selected, and the samples were denoted as PMMA-6 and PMMA-12, respectively. No chemical compatibilizers were used to avoid introducing additional variables affecting degradation behavior. This approach enables a direct evaluation of the influence of mixing time and physical dispersion on the thermal response of the nanocomposites and is consistent with established processing methodologies reported for polymer–nanoparticle systems [19,20].

2.3. Differential Thermal Analysis (DTA) (Diferansiyel Termal Analiz (DTA))

Differential thermal analysis (DTA) and thermogravimetric analysis (TGA) were conducted to evaluate the thermal degradation behavior and stability of PMMA and PMMA/NiFe₂O₄ nanocomposites. Measurements were performed using a Hitachi Exstar SII 7300 simultaneous thermal analyzer (Hitachi, Tokyo, Japan) under a controlled nitrogen atmosphere. Approximately 5 ± 0.5 mg of each sample was placed in alumina crucibles to ensure uniform heat transfer conditions.

Thermal analyses were carried out at heating rates (β) of 5, 10, 15, and 20 K·min⁻¹ over a temperature range up to 1000 K to capture the complete degradation process. A constant nitrogen flow rate of 50 mL·min⁻¹ was maintained throughout the experiments to prevent oxidative effects. The onset temperature (T_0) and the maximum degradation temperature (T_x) were determined from the DTA curves to evaluate the influence of NiFe₂O₄ incorporation and mixing time on thermal stability [21]. Based on the non-isothermal DTA/TGA data obtained at different heating rates, kinetic parameters were calculated using the Kissinger, Takhor, and Augis–Bennett methods to determine the apparent activation energy (E_a) of degradation. Pure PMMA was analyzed under identical

conditions to serve as a reference material. Prior to measurements, the instrument was calibrated using standard alumina crucibles. All experiments were performed in triplicate to ensure reproducibility and accuracy.

2.4. Kinetic Analysis of Thermal Degradation (Termal Bozunmanın Kinetik Analizi)

The thermal degradation kinetics of PMMA and PMMA/NiFe₂O₄ nanocomposites were evaluated using non-isothermal kinetic methods. Activation energies were calculated based on the characteristic temperatures obtained from DTA analysis at different heating rates. The Kissinger, Ozawa, and Augis–Bennett methods were applied to determine the apparent activation energies associated with the main degradation stage [22–24].

These methods are widely used for kinetic analysis of polymer degradation processes and provide reliable comparative information regarding the effect of fillers and processing conditions on thermal stability. The consistency of the results obtained from different kinetic models was used to validate the reliability of the calculated activation energy values [23,25].

2.5. SEM Analysis (SEM Analizi)

Scanning electron microscopy (SEM) analyses were carried out using a SEM model (JEOL JSM-6064LV) operated at an accelerating voltage of 10 kV. Samples were prepared by fracturing the specimens in liquid nitrogen to obtain representative cross-sections, followed by sputter coating with a thin layer of gold to avoid charging effects. Quantitative image analysis was performed using image analysis software (ImageJ). Agglomerates were defined as particle clusters with an area larger than approximately 0.1 μm^2 , and the analysis was conducted as a comparative trend evaluation due to limited SEM fields.

2.6. X-Ray Diffraction (XRD) Analysis (X-ışını Kırınımı (XRD) Analizi)

Phase composition and structural characteristics of PMMA and PMMA/NiFe₂O₄ nanocomposites were analyzed using a Bruker D8 Advance X-ray diffractometer (Bruker, Billerica, MA, USA) equipped with CuK α radiation ($\lambda = 0.154056$ nm). Diffraction patterns were recorded in the 2θ range of 5–80° with a step size of 0.013° to ensure high-resolution data acquisition. The measurements were carried out at room temperature under standard operating conditions. The obtained diffraction patterns were used to evaluate the amorphous nature

of the PMMA matrix and to identify the characteristic crystalline reflections of NiFe_2O_4 nanoparticles.

3. RESULTS AND DISCUSSION (BULGULAR VE TARTIŞMA)

3.1. XRD Characterization (XRD Karakterizasyonu)

The structural characteristics of PMMA and PMMA/ NiFe_2O_4 nanocomposites were investigated by X-ray diffraction (XRD) analysis. The XRD patterns of PMMA, PMMA-6, and PMMA-12 samples are presented in Figure 1. As observed, pure PMMA exhibits a broad diffraction halo centered in the range of $2\theta \approx 15\text{--}25^\circ$, confirming its amorphous structure. This characteristic amorphous diffraction behavior of PMMA has been widely reported in the literature [12,17]. The XRD patterns of PMMA-6 and PMMA-12 samples remain largely unchanged after the incorporation of NiFe_2O_4 nanoparticles, indicating that the amorphous nature of the PMMA matrix is preserved. Similar observations have been reported for PMMA-based nanocomposites reinforced with inorganic fillers,

where no crystallization of the polymer matrix occurs [2,3].

Weak diffraction peaks corresponding to the characteristic planes of NiFe_2O_4 can be identified in the nanocomposite samples, confirming the presence of the ferrite phase within the polymer matrix. The absence of peak shifting or additional diffraction peaks suggests that the interaction between PMMA and NiFe_2O_4 nanoparticles is predominantly physical rather than chemical [18,20]. Furthermore, no significant difference is observed between the XRD patterns of PMMA-6 and PMMA-12, indicating that variation in mixing time does not alter the structural characteristics of the polymer matrix. As shown in Figure 1, the broad amorphous halo of PMMA is preserved for both PMMA-6 and PMMA-12 samples, indicating that variations in mixing time affect neither the structural nature nor the amorphous character of the polymer matrix.

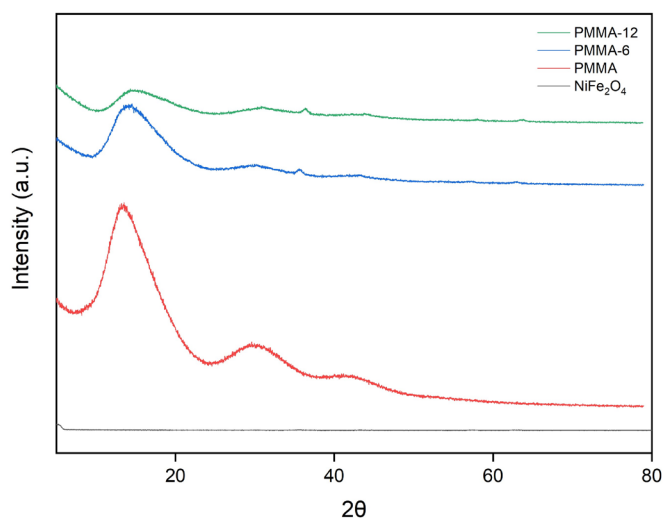


Figure 1. XRD patterns of NiFe_2O_4 , PMMA, PMMA-6, and PMMA-12 samples (NiFe_2O_4 , PMMA, PMMA-6 ve PMMA-12 numunelerinin XRD desenleri)

3.2. Morphological Analysis by SEM (SEM ile Morfolojik Analiz)

The dispersion state of NiFe_2O_4 nanoparticles within the PMMA matrix was examined by scanning electron microscopy (SEM). SEM micrographs of PMMA, PMMA-6, and PMMA-12 samples are shown in Figure 2(a–c).

The SEM image of pure PMMA (Figure 2a) reveals smooth and homogeneous surface morphology, which is typical for amorphous polymer matrices [1]. In contrast, the PMMA-6 sample (Figure 2b) exhibits localized regions containing nanoparticle agglomerates dispersed within the polymer matrix. Such agglomeration leads to microstructural heterogeneities that may restrict polymer chain mobility and influence thermal degradation behavior [4,20]. The SEM micrograph of PMMA-

12 (Figure 2c) demonstrates a more uniform distribution of NiFe₂O₄ nanoparticles throughout the PMMA matrix. The improved dispersion observed in PMMA-12 can be attributed to the extended mixing time, which promotes the breakup of nanoparticle clusters and increases the effective polymer–particle interfacial area. Similar dispersion dependent morphological behavior has been reported for polymer nanocomposites processed under optimized mixing conditions [5,7]. These morphological differences play a critical role in governing the thermal response and degradation kinetics of the nanocomposites, as discussed in the following sections. As illustrated in Figure 2, increasing the mixing time leads to a noticeable transition from localized nanoparticle agglomeration (PMMA-6) to a more homogeneous

dispersion state (PMMA-12). These distinct morphological features are expected to impose different levels of interfacial constraint on polymer chain mobility, which is a key factor influencing thermal degradation kinetics.

Quantitative SEM analysis performed at 2000× magnification revealed distinct dispersion characteristics between PMMA-6 and PMMA-12 samples. PMMA-6 exhibited fewer but larger agglomerates with a broader size distribution, whereas PMMA-12 showed a higher number density of smaller and more uniformly distributed agglomerates, reflecting enhanced dispersion resulting from prolonged mixing. The corresponding quantitative parameters are summarized in Table 1.

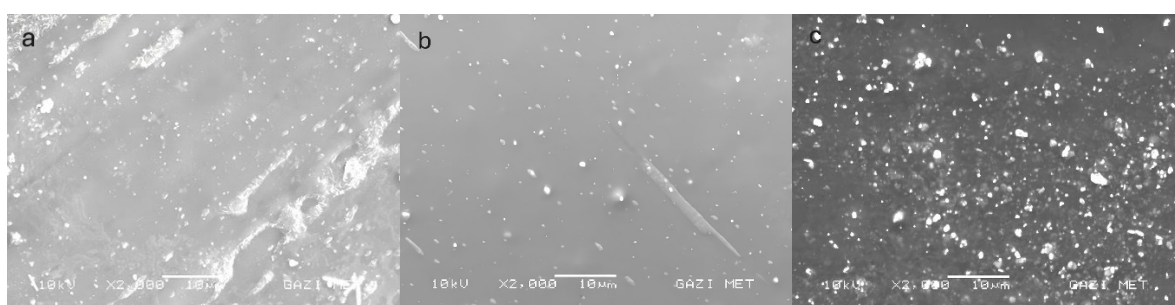


Figure 2. SEM images of (a) PMMA, (b) PMMA-6, and (c) PMMA-12 samples. ((a) PMMA, (b) PMMA-6 ve (c) PMMA-12 örneklerinin SEM görüntüleri)

Table 1. Quantitative SEM analysis of agglomerate characteristics (Topaklanma özelliklerinin nicel SEM analizi)

Sample	Number of agglomerates (n)	Mean area (µm ²)	Std. dev. (µm ²)	Coefficient of Variation (CV) (%)	Equivalent diameter (µm)
PMMA-6	28	0.34	0.48	141	0.66
PMMA-12	42	0.19	0.21	110	0.49

The quantitative parameters summarized in Table 1 further support the qualitative SEM observations. PMMA-6 exhibits fewer but larger agglomerates with a broader size distribution, whereas PMMA-12 shows a higher density of smaller agglomerates, confirming enhanced dispersion with prolonged mixing. In recent studies, it has been emphasized that an intermediate dispersion state, characterized by partial nanoparticle agglomeration together with strong polymer–particle interactions, may lead to maximum restriction of polymer chain mobility and enhanced thermal resistance [20,21]. This behavior is consistent with the present results, where the PMMA-6 sample exhibits a higher activation energy despite less homogeneous dispersion compared to PMMA-12. Such findings highlight that optimal, rather than maximum, dispersion governs the thermal degradation kinetics of polymer nanocomposites.

3.3. Thermal Degradation Behavior (Termal Bozunma Davranışı)

The thermal degradation behavior of PMMA and PMMA/NiFe₂O₄ nanocomposites was investigated by differential thermal analysis (DTA) at different heating rates. The DTA curves of pure PMMA, PMMA-6, and PMMA-12 at various heating rates (5, 10, 15, and 20 K/min) are shown in Figure 3a–c. As shown in Figure 3, all samples exhibit a single dominant degradation peak, indicating a similar overall degradation mechanism. However, subtle differences in peak shape and thermal response suggest that nanoparticle dispersion primarily affects degradation kinetics rather than the characteristic degradation temperature.

All samples exhibit a single dominant endothermic peak corresponding to the main thermal degradation stage of PMMA, indicating that the incorporation of NiFe₂O₄ nanoparticles does not alter the

fundamental degradation mechanism of the polymer matrix. Similar degradation behavior has been reported for PMMA-based nanocomposites containing inorganic fillers [8,9]. The characteristic

degradation parameters, including onset temperature (T_o) and maximum degradation temperature (T_x), are summarized in Table 2.

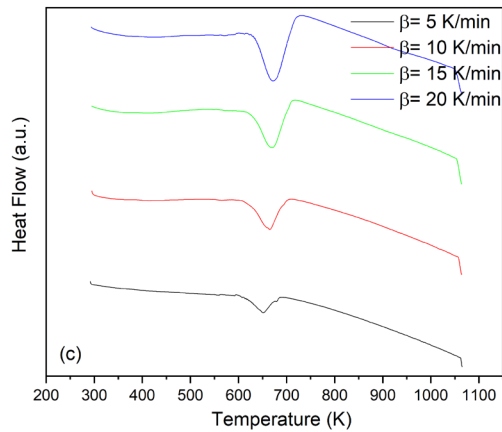
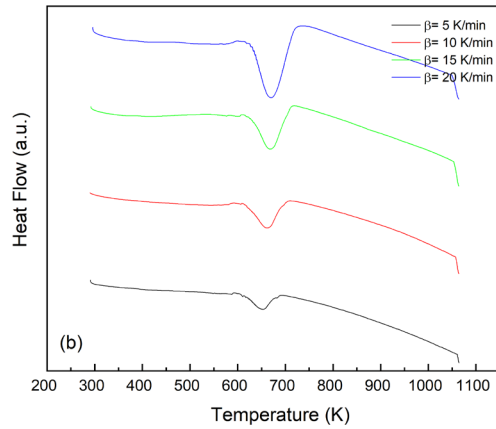
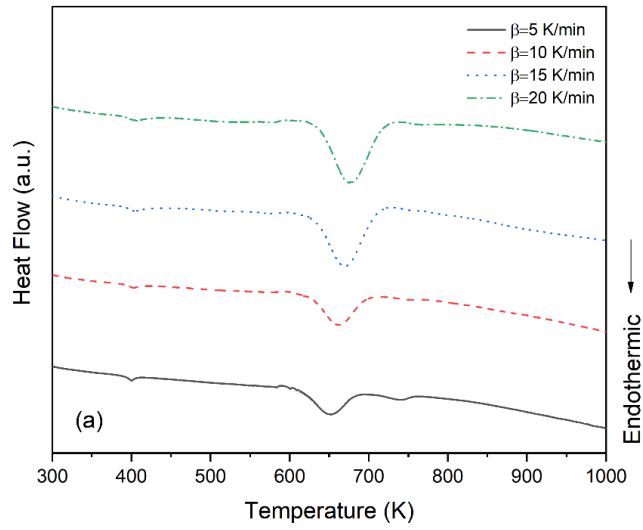


Figure 3. DTA curves of the samples (a) PMMA, (b) PMMA-6 and (c) PMMA-12. ((a) PMMA, (b) PMMA-6 ve (c) PMMA-12 örneklerinin DTA eğrileri)

Table 3. Thermal analysis results of PMMA, PMMA-6, and PMMA-12 samples (PMMA, PMMA-6 ve PMMA-12 numunelerinin Termal analiz sonuçları)

SAMPLES	β (K/min)	T_o (K)	T_x (K)	A
PMMA	5	590	651	266
	10	593	661	279
	15	595	670	311
	20	597	676	281
PMMA-6	5	592	653	331
	10	608	661	325
	15	609	668	323
	20	607	670	447
PMMA-12	5	594	651	332
	10	600	665	336
	15	601	670	342
	20	616	672	356

According to Table 2, the T_x values of PMMA-6 and PMMA-12 are comparable to those of pure PMMA at all heating rates. This indicates that the addition of NiFe₂O₄ nanoparticles and the variation in mixing time have a limited effect on the degradation temperature. However, differences in the shape and stability of the DTA curves are evident. PMMA-6 shows slight irregularities at the onset of degradation, whereas PMMA-12 exhibits smoother thermal behavior, which can be attributed to differences in nanoparticle dispersion. Recent investigations on PMMA-based nanocomposites have shown that the incorporation of metal oxide and ferrite nanoparticles may not significantly shift degradation temperatures but can markedly alter degradation pathways and reaction rates [1]. The present results support this observation, as the T_x values remain nearly unchanged while notable differences are observed in the degradation kinetics and activation energies of the samples.

The broader agglomerate size distribution observed in PMMA-6 suggests the presence of controlled particle clustering, which may induce heterogeneous restriction of polymer chain mobility. This morphological feature is consistent with the higher activation energies obtained for PMMA-6 from Kissinger, Ozawa, and Augis–Bennett analyses.

In contrast, the finer and more homogeneous dispersion observed in PMMA-12, while indicative of improved particle distribution, may reduce localized interfacial constraints, leading to lower effective energy barriers for thermal degradation.

3.4. Effect of Heating Rate (Isıtma Hızının Etkisi)

The activation energies of the samples were calculated from the DTA curves by analyzing the thermal events associated with the degradation process. Additionally, the Avrami parameter (n) was determined from the degradation peaks, providing important insights into microstructural changes within the nanocomposites. According to the literature, the Avrami parameter helps characterize the nucleation and growth mechanism, indicating whether these processes occur superficially or volumetrically, as well as the dimensionality of growth from the surface inward. The Avrami parameters were derived from the slopes of the linear fits based on the Ozawa equation. Figure 4 illustrates the plots of $\ln[-\ln(1-\phi)]$ versus $\ln(\beta)$ for PMMA, PMMA-6, and PMMA-12 samples, calculated in accordance with the Ozawa method. The linear relationships observed in the Ozawa plots (Figure 4) confirm the validity of non-isothermal kinetic analysis for all samples. The Avrami parameter values close to unity indicate a surface-controlled degradation process, suggesting that nanoparticle incorporation and dispersion state modify the energy barrier without altering the fundamental degradation mechanism. The invariance of the Avrami parameter across all samples, combined with the observed differences in activation energy, indicates that nanoparticle dispersion modifies the energetic landscape of degradation without altering the dominant degradation pathway.

The Avrami parameter values close to unity ($n \approx 1$) indicate a surface-controlled degradation process dominated by random chain scission. The invariance of the Avrami parameter across all samples confirms that nanoparticle incorporation

modifies the energetic barrier of degradation without altering the fundamental degradation mechanism [23,24]. The invariance of the Avrami parameter upon NiFe₂O₄ incorporation and varying dispersion states indicates that the fundamental degradation pathway of PMMA remains unchanged. Instead, the nanoparticles primarily modify the energetic barrier of degradation rather than altering the degradation mechanism itself. This behavior is consistent with recent studies on polymer nanocomposites, where the addition of inorganic nanoparticles increased activation energy while preserving surface-controlled degradation characteristics. Therefore, the constant Avrami parameter combined with varying activation energy values confirms that NiFe₂O₄ nanoparticles act as

kinetic stabilizers rather than mechanism modifiers in the thermal degradation of PMMA [24].

The effect of heating rate on the thermal degradation behavior of the samples was examined by performing DTA measurements at heating rates of 5, 10, 15, and 20 K/min. The variation of T_x with heating rate is shown in Figure 4. This suggests that the incorporation of NiFe₂O₄ nanoparticles and variations in dispersion state primarily affect the energetic barrier of degradation rather than altering the fundamental degradation pathway of PMMA. The invariance of the Avrami parameter further confirms that nanoparticle dispersion modifies degradation kinetics without inducing a change in the degradation mechanism.

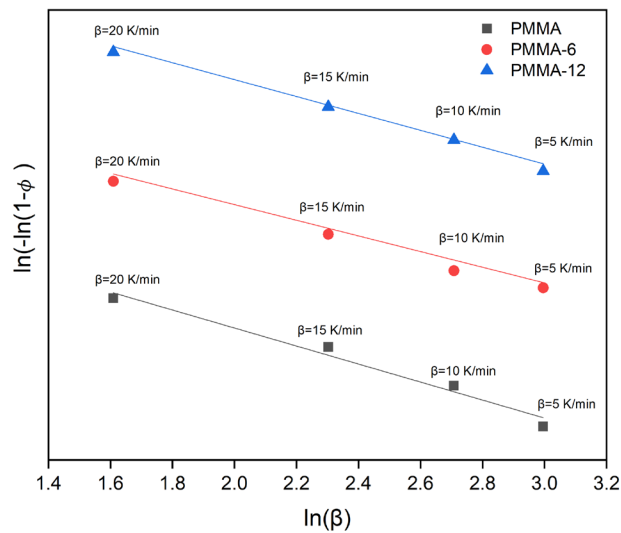


Figure 4. Ozawa plots for PMMA, PMMA-6 and PMMA-12 samples (PMMA, PMMA-6 ve PMMA-12 numuneleri için Ozawa grafikleri)

For all samples, T_x shifts toward higher temperatures with increasing heating rate, which is a typical feature of non-isothermal thermal analysis. This behavior is attributed to thermal lag and reduced reaction time at higher heating rates [13–15]. The similar trends observed for PMMA and nanocomposite samples indicate that the fundamental degradation mechanism remains unchanged.

3.5. Thermal Degradation Kinetics (Termal Bozunma Kinetiği)

The thermal degradation kinetics of PMMA and PMMA/NiFe₂O₄ nanocomposites were evaluated using Kissinger, Ozawa, and Augis–Bennett methods based on DTA data obtained at different

heating rates. The corresponding kinetic plots are presented in Figure 5.

As evidenced by the kinetic plots shown in Figures 5–7, PMMA-6 consistently exhibits higher slopes compared to PMMA and PMMA-12, corresponding to increased activation energy values. This behavior demonstrates that an optimum dispersion state characterized by partial agglomeration provides more effective restriction of polymer chain mobility than a fully homogeneous nanoparticle distribution. In addition to absolute activation energy values, the steeper slopes observed for PMMA-6 in the Kissinger, Ozawa, and Augis–Bennett plots indicate a higher sensitivity of the degradation rate to temperature, reflecting the presence of a more pronounced energy barrier for chain scission. The

calculated activation energy values are summarized in Table 3.

Notably, all three non-isothermal kinetic methods yield a consistent activation energy trend (PMMA-

6 > PMMA-12 > PMMA), indicating that the observed differences are intrinsic to the degradation behavior of the system rather than artifacts arising from the mathematical assumptions of individual kinetic models.

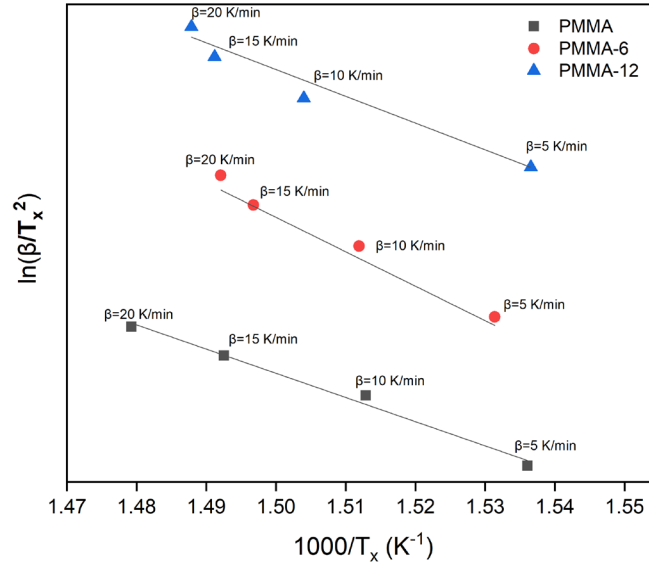


Figure 5. $\ln(\beta/T_x^2)$ - $1000/T_x$ plot for PMMA, PMMA-6 and PMMA-12 samples according to Kissinger Formula (Kissinger Formülüne göre PMMA, PMMA-6 ve PMMA-12 örnekleri için $\ln(\beta/T_x^2)$ - $1000/T_x$ grafiği)

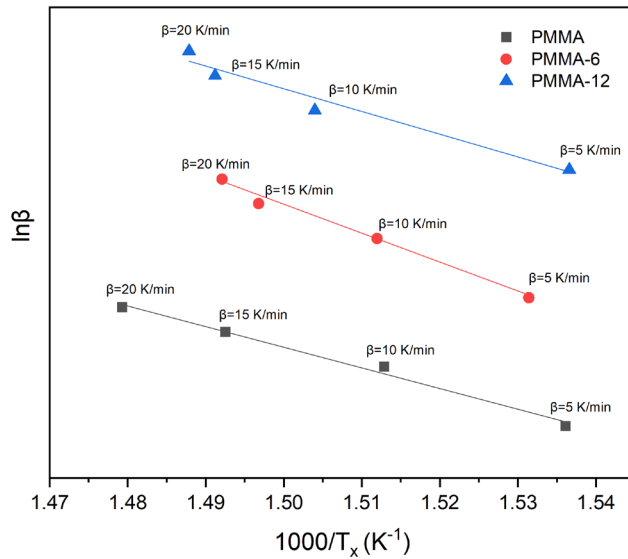


Figure 6. $\ln \beta$ - $1000/T_x$ graph for PMMA, PMMA-6, and PMMA-12 samples according to Ozawa Formula ($\ln \beta$ - $1000/T_x$ graph for PMMA, PMMA-6, and PMMA-12 samples according to Ozawa Formula)

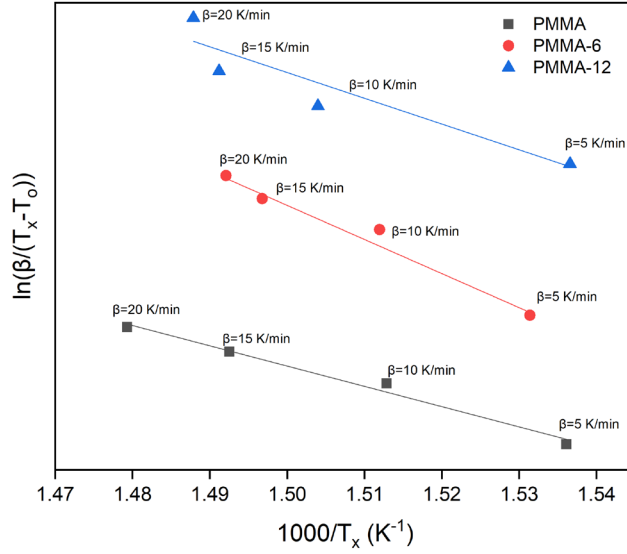


Figure 7. $\ln(\beta/T_x-T_o)-1000/T_x$ chart for samples according to Augis-Bennett Formula (Augis-Bennett Formülüne göre örnekler için $\ln(\beta/T_x-T_o)-1000/T_x$ grafiği)

Table 3. Activation energies calculated from the values of the samples as a result of DTA (DTA verilerinden elde edilen değerler kullanılarak hesaplanan aktivasyon enerjileri)

Samples	Avrami Parameter	Kissinger Method (kJ/Mol)	Ozawa Method (kJ/Mol)	Augis-Bennett Method (kJ/Mol)
PMMA	1	189	200	162
PMMA-6	1	270	280	273
PMMA-12	1	210	221	206

Recent studies have shown that maximum nanoparticle dispersion does not always result in maximum thermal stability in polymer nanocomposites. Instead, an optimum dispersion state—often involving partial nanoparticle agglomeration—can enhance thermal resistance by forming constrained polymer regions around filler clusters. These constrained regions limit polymer chain mobility and increase the energy barrier required for thermal degradation [25,26].

In a recent study by Ulutaş (2025), the effect of mixing time on the thermal degradation behavior of metal oxide–reinforced PMMA nanocomposites was systematically investigated. It was demonstrated that nanocomposites processed under intermediate mixing conditions exhibited higher activation energies compared to both neat PMMA and samples subjected to prolonged mixing, highlighting the presence of an optimum dispersion regime rather than a fully homogeneous distribution [27].

Similar observations have been reported in recent literature, where partially agglomerated nanofiller structures were found to impose stronger local interfacial constraints on polymer chains than fully dispersed systems, resulting in improved thermal stability and higher degradation activation energies [26,28].

In the present study, the PMMA-6 sample exhibits such an optimum dispersion state. The partial agglomeration of NiFe₂O₄ nanoparticles enhances polymer–particle interfacial interactions without altering the amorphous structure of the PMMA matrix, leading to the highest activation energy among the investigated samples. These findings confirm that optimum, rather than maximum, nanoparticle dispersion governs the thermal degradation kinetics of PMMA/NiFe₂O₄ nanocomposites.

Pure PMMA exhibits an activation energy consistent with values reported in the literature

[8,21]. The incorporation of NiFe₂O₄ nanoparticles results in an increase in activation energy, indicating enhanced resistance to thermal degradation. Among the nanocomposites, PMMA-6 exhibits the highest activation energy, suggesting that partial nanoparticle agglomeration combined with strong polymer–particle interactions effectively restricts polymer chain mobility [4,5]. In contrast, PMMA-12 shows a lower activation energy compared to PMMA-6, despite improved nanoparticle dispersion. This indicates that maximum dispersion does not necessarily correspond to maximum thermal resistance, and that an optimum dispersion state governs the degradation kinetics of PMMA-based nanocomposites. Although PMMA-12 exhibits a more homogeneous nanoparticle dispersion, its lower activation energy compared to PMMA-6 suggests that excessive dispersion may reduce localized interfacial constraints, thereby facilitating segmental polymer chain motion and lowering the effective energy barrier for thermal degradation.

Similar trends have also been observed in non-isothermal kinetic studies, where partially agglomerated nanofiller structures were reported to increase activation energy by inducing constrained polymer regions around filler clusters [20,22]. These findings demonstrate that, for PMMA/NiFe₂O₄ nanocomposites, maximum nanoparticle dispersion does not necessarily lead to maximum thermal resistance. Instead, an optimum dispersion state characterized by partial agglomeration and strong interfacial constraint governs the degradation kinetics. The convergence of kinetic parameters derived from different analytical approaches highlights the reliability of DTA-based non-isothermal analysis for comparative evaluation of dispersion effects in PMMA-based nanocomposites. This consistency reinforces the validity of correlating morphological features with degradation kinetics.

4. CONCLUSIONS (SONUÇLAR)

In this study, the structural, morphological, and thermal degradation behavior of PMMA and PMMA/NiFe₂O₄ nanocomposites prepared with different mixing times were systematically investigated using XRD, SEM, and non-isothermal DTA analyses. The combined results provide a comprehensive understanding of the role of nanoparticle dispersion and processing conditions on the thermal stability and degradation kinetics of PMMA-based nanocomposites. XRD analysis confirmed that the incorporation of NiFe₂O₄ nanoparticles did not alter the amorphous structure

of the PMMA matrix, regardless of mixing time. The absence of significant structural changes indicates that the observed variations in thermal behavior originate primarily from morphological and interfacial effects rather than crystallinity differences. SEM observations revealed that mixing time plays a critical role in controlling nanoparticle dispersion within the PMMA matrix. While the PMMA-6 sample exhibited partial nanoparticle agglomeration, PMMA-12 showed a more homogeneous dispersion. These morphological differences were found to directly influence the thermal degradation behavior and kinetic parameters of the nanocomposites.

DTA results demonstrated that the main degradation temperatures of PMMA remained largely unchanged upon NiFe₂O₄ incorporation. However, significant differences were observed in the degradation kinetics. Kinetic analyses based on Kissinger, Ozawa, and Augis–Bennett methods revealed that the PMMA-6 nanocomposite exhibited the highest activation energy among the investigated samples. This behavior was attributed to an optimum dispersion state characterized by partial agglomeration combined with strong polymer–particle interactions, which effectively restrict polymer chain mobility and increase the energy barrier for thermal degradation. In contrast, although PMMA-12 exhibited improved nanoparticle dispersion, its activation energy was lower than that of PMMA-6, indicating that over-processing or excessive dispersion may be energetically inefficient for achieving optimal thermal performance. These findings highlight that an optimum dispersion state, rather than complete homogeneity, governs the thermal degradation kinetics of PMMA/NiFe₂O₄ nanocomposites.

Overall, this study demonstrates that controlled processing parameters, particularly mixing time, can be effectively used to tailor the thermal degradation behavior and kinetic response of PMMA-based nanocomposites without altering their structural characteristics. The results provide valuable insights for the design of polymer nanocomposites with enhanced thermal performance and controlled degradation behavior for advanced engineering applications. The present study is limited to a fixed nanoparticle concentration and two mixing durations. Future studies may focus on different filler loadings, surface-modified nanoparticles, and complementary thermal analysis techniques to further elucidate dispersion-controlled degradation mechanisms.

DECLARATION OF ETHICAL STANDARDS (ETİK STANDARTLARIN BEYANI)

The author of this article declares that the materials and methods they use in their work do not require ethical committee approval and/or legal-specific permission.

Bu makalenin yazarı çalışmalarında kullandıkları materyal ve yöntemlerin etik kurul izni ve/veya yasal-özel bir izin gerektirmediğini beyan ederler.

AUTHORS' CONTRIBUTIONS (YAZARLARIN KATKILARI)

Aytekin ULUTAŞ: He conducted the experiments, analyzed the results and performed the writing process.

Deneyleri yapmış, sonuçlarını analiz etmiş ve maklenin yazım işlemini gerçekleştirmiştir.

CONFLICT OF INTEREST (ÇIKAR ÇATIŞMASI)

There is no conflict of interest in this study.

Bu çalışmada herhangi bir çıkar çatışması yoktur.

REFERENCES (KAYNAKLAR)

- [1] Gałko G, Sajdak M. Trends for the thermal degradation of polymeric materials: analysis of available techniques, issues, and opportunities. *Applied Sciences*. 2022; 12: 9138. <https://doi.org/10.3390/app12189138>
- [2] Praveena, B. A., Buradi, A., Santhosh, N., Vasu, V. K., Hatgundi, J., & Huliya, D. Study on characterization of mechanical, thermal properties, machinability and biodegradability of natural fiber reinforced polymer composites and its applications, recent developments and future potentials: A comprehensive review. *Materials Today: Proceedings*. 2022. <https://doi.org/10.1016/j.matpr.2021.11.049>
- [3] Ramesh M, Rajeshkumar LN, Srinivasan N, Kumar DV, Balaji D. Influence of filler material on properties of fiber-reinforced polymer composites: a review. *e-Polymers*. 2022; 22: 898–916. <https://doi.org/10.1515/epoly-2022-0061>
- [4] Yesaswi CS, Satya SK, Sahu SK, Badgayan ND, Murthy PSR, Kumar VR, Sreekanth PR. Thermal properties of polymer nanocomposites. In: *Advanced Polymer Nanocomposites*. Woodhead Publishing. 2022; 99–143. <https://doi.org/10.1016/B978-0-12-824273-8.00005-6>
- [5] Mohammed MI, Moustapha ME, Gomaa F. Comprehensive characterization of NiO/PMMA polymeric nanocomposite films: physicochemical, thermal, optical, and photocatalytic properties. *Polymers for Advanced Technologies*. 2025; 36: e70352. <https://doi.org/10.1002/pat.70352>
- [6] Xie Z, Liu D, Xiao Y, Wang K, Zhang Q, Wu K, Fu Q. The effect of filler permittivity on the dielectric properties of polymer-based composites. *Composites Science and Technology*. 2022; 222: 109342. <https://doi.org/10.1016/j.compscitech.2022.109342>
- [7] Ragab HM, Diab NS, Aleid GM, Alghamdi AM, Al-Sagheer LAM, Farea MO. Enhancement of structural, optical, and electrical properties of hydroxypropyl methylcellulose/polyvinyl alcohol nanocomposites by nickel ferrite nanoparticles for optoelectronic applications. *Journal of Inorganic and Organometallic Polymers and Materials*. 2025; 35: 1152–1164. <https://doi.org/10.1007/s10904-024-03337-4>
- [8] Svobodova-Sedlackova A, Huete-Hernandez S, Calderón A, Barreneche C, Gamallo P, Fernandez AI. Effect of nanoparticles on the thermal stability and reaction kinetics in ionic nanofluids. *Nanomaterials*. 2022; 12: 1777. <https://doi.org/10.3390/nano12101777>
- [9] Alhotan A, Elraggal A, Yates J, Haider J, Jurado CA, Silikas N. Effect of different solutions on the colour stability of nanoparticles or fibre reinforced PMMA. *Polymers*. 2022; 14: 1521. <https://doi.org/10.3390/polym14081521>
- [10] Chen XG, Zhang YF. Thermal, mechanical and electrical properties of Ag nanoparticle–polymethyl methacrylate composites under different service temperatures. *Journal of Composites Science*. 2024; 8: 279. <https://doi.org/10.3390/jcs8070279>
- [11] Munir KS, Li Y, Liang D, Qian M, Xu W, Wen C. Effect of dispersion method on the deterioration, interfacial interactions and re-agglomeration of carbon nanotubes in titanium metal matrix composites. *Materials & Design*. 2015; 88: 138–148. <https://doi.org/10.1016/j.matdes.2015.08.108>
- [12] López D, Cendoya I, Torres F, Tejada J, Mijangos C. Thermal transitions in polymer systems. *Journal of Applied Polymer Science*. 2001; 82: 3215–3222. <https://doi.org/10.1002/app.2180>
- [13] Ozawa T. A new method of analyzing thermogravimetric data. *Bulletin of the Chemical Society of Japan*. 1965; 38: 1881–1886.

- <https://doi.org/10.1246/bcsj.38.1881>
- [14] Kissinger HE. Reaction kinetics in differential thermal analysis. *Analytical Chemistry*. 1957; 29: 1702–1706.
<https://doi.org/10.1021/ac60131a045>
- [15] Singh P, Kumar R, Virk HS, Prasad R. Thermal properties of polymeric materials. *Indian Journal of Pure and Applied Physics*. 2010; 48: 321–324.
- [16] Yanmaz E, Doğan M, Turhan Y. Thermal and mechanical behavior of carbon-based composites. *Diamond and Related Materials*. 2021; 115: 108359.
<https://doi.org/10.1016/j.diamond.2021.108359>
- [17] Porter CE, Blum FD. Thermal characterization of PMMA thin films using modulated differential scanning calorimetry. *Macromolecules*. 2000; 33: 7016–7020.
<https://doi.org/10.1021/ma000302l>
- [18] Elashmawi IS, Ismail AM. Study of the spectroscopic, magnetic, and electrical behavior of PVDF/PEO blend incorporated with nickel ferrite (NiFe₂O₄) nanoparticles. *Polymer Bulletin*. 2022; 80: 2329–2348.
<https://doi.org/10.1007/s00289-022-04139-9>
- [19] Martin C. Twin screw extruders as continuous mixers for thermal processing: a technical and historical perspective. *AAPS PharmSciTech*. 2016; 17: 3–19.
<https://doi.org/10.1208/s12249-016-0485-3>
- [20] Rishi K, Narayanan V, Beaucage G, McGlasson A, Kuppa V, Ilavsky J, Rackaitis M. A thermal model to describe kinetic dispersion in rubber nanocomposites: The effect of mixing time on dispersion. *Polymer*. 2019; 175: 272–282.
<https://doi.org/10.1016/j.polymer.2019.03.044>
- [21] Cho YM, Kim JH, Choi JH, Kim JC, Cho SM, Park SW, Kwak HW, Choi IG. Physicochemical characteristics of lignin-g-PMMA/PLA blend via atom transfer radical polymerization depending on the structural difference of organosolv lignin. *International Journal of Biological Macromolecules*. 2023; 226: 279–290.
<https://doi.org/10.1016/j.ijbiomac.2022.11.316>
- [22] Yassin AY, Salem A, Asnag GM, Al-Muntaser AA, Alanazi FK, Almarri HM, Alshehri NA, Abdallah EM. Reinforcing the structural, optical and dielectric properties through the integration of CuO nanoparticles into PS/PMMA: NiFe₂O₄ electrolyte. *Journal of Materials Science: Materials in Electronics*. 2025; 36: 1692.
<https://doi.org/10.1007/s10854-025-15704-z>
- [23] Baloch MK, Khurram MJZ, Durrani GF. Application of different methods for the thermogravimetric analysis of polyethylene samples. *Journal of Applied Polymer Science*. 2011; 120: 3511–3518.
<https://doi.org/10.1002/app.33447>
- [24] Vyazovkin S, Galukhin A. Problems with applying the Ozawa–Avrami crystallization model to non-isothermal crosslinking polymerization. *Polymers*. 2022; 14: 693.
<https://doi.org/10.3390/polym14040693>
- [25] Choudhury A, Bhowmick AK, Ong C, Soddemann M. Effect of various nanofillers on thermal stability and degradation kinetics of polymer nanocomposites. *Journal of Nanoscience and Nanotechnology*. 2010; 10: 5056–5071.
<https://doi.org/10.1166/jnn.2010.3030>
- [26] Kausar A, Bocchetta P. Poly(methyl methacrylate) nanocomposite foams reinforced with carbon and inorganic nanoparticles: state-of-the-art. *Journal of Composites Science*. 2022; 6: 129.
<https://doi.org/10.3390/jcs6050129>
- [27] Ulutaş A. Effect of mixing time on the thermal stability and activation energies of metal oxide/PMMA nanocomposites. *Journal of Composites Science*. 2025; 9: 557.
<https://doi.org/10.3390/jcs9100557>
- [28] Maleki FK, Nasution MK, Gok MS, Maleki VA. An experimental investigation on mechanical properties of Fe₂O₃ microparticles reinforced polypropylene. *Journal of Materials Research and Technology*. 2022; 16: 229–237.
<https://doi.org/10.1016/j.jmrt.2021.11.104>